Virus Research 339 (2024) 199250

Contents lists available at ScienceDirect

Virus Research

journal homepage: www.elsevier.com/locate/virusres

The lncRNA MEG3/miRNA-21/P38MAPK axis inhibits coxsackievirus 3 replication in acute viral myocarditis

Feng He [a,1], Zhuo Liu [a,1], Miao Feng [a], Zonghui Xiao [a], Xiaoyu Yi [a], Jianxin Wu [a,b,c], Zhewei Liu [a], Gaoyu Wang [d], Le Li [d,*], Hailan Yao [a,*]

[a] Department of Biochemistry and Immunology, Capital Institute of Pediatrics, YaBaoRoad 2, Beijing, China
[b] Beijing Municipal Key Laboratory of Child Development and Nutriomics, Beijing, China
[c] Beijing Tongren Hospital, Capital Medical University, Beijing, China
[d] NHC Key Laboratory of Tropical Disease Control, Hainan Medical University, Haikou, China

ARTICLE INFO

Keywords:
Coxsackievirus 3
lncRNA
miRNA
P38MAPK
Viral replication

ABSTRACT

Evidence is emerging on the roles of long noncoding RNAs (lncRNAs) as regulatory factors in a variety of viral infection processes, but the mechanisms underlying their functions in coxsackievirus group B type3 (CVB3)-induced acute viral myocarditis have not been explicitly delineated. We previously demonstrated that CVB3 infection decreases miRNA-21 expression; however, lncRNAs that regulate the miRNA-21-dependent CVB3 disease process have yet to be identified. To evaluate lncRNAs upstream of miRNA-21, differentially expressed lncRNAs in CVB3-infected mouse hearts were identified by microarray analysis and lncRNA/miRNA-21 interactions were predicted bioinformatically. MEG3 was identified as a candidate miRNA-21-interacting lncRNA upregulated in CVB3-infected mouse hearts. MEG3 expression was verified to be upregulated in HeLa cells 48 h post CVB3 infection and to act as a competitive endogenous RNA of miRNA-21. MEG3 knockdown resulted in the upregulation of miRNA-21, which inhibited CVB3 replication by attenuating P38-MAPK signaling *in vitro* and *in vivo*. Knockdown of MEG3 expression before CVB3 infection inhibited viral replication in mouse hearts and alleviated cardiac injury, which improved survival. Furthermore, the knockdown of CREB5, which was predicted bioinformatically to function upstream of MEG3, was demonstrated to decrease MEG3 expression and CVB3 viral replication. This study identifies the function of the lncRNA MEG3/miRNA-21/P38 MAPK axis in the process of CVB3 replication, for which CREB5 could serve as an upstream modulator.

1. Introduction

Coxsackievirus group B type3 (CVB3) is a positive-stranded RNA virus belonging to the picornaviridae family that has been well-established as the leading causative agent of acute and chronic myocarditis and has also been associated with pancreatitis and meningitis, especially in infants and teenagers (Kaplan et al., 1983; Kim et al., 2001; Ozsvár et al., 1992; Rorabaugh et al., 1993; Tracy et al., 2000). Viral infection is associated with transcriptional alterations of the host, including changes in the expression of genes that participate in important biological or pathological processes, such as antiviral responses, apoptosis, autophagy, inflammation, and necrosis (Rassmann et al., 2013). Viral infection is also known to alter the expression of noncoding RNAs, including microRNAs (miRNAs), small nuclear RNAs (snRNAs), long noncoding RNAs (lncRNAs), Piwi-interacting RNAs (piRNAs), and circular RNAs (circRNAs), which have been reported to facilitate viral replication or participate in apoptosis, proliferation, metabolism or antiviral immunity (Ballinger et al., 2022; Lai et al., 2021; Wang et al., 2022; Zhang et al., 2018).

Generally, LncRNAs are defined as RNA transcripts of more than 200 nt in length that lack protein-coding potential (Aryankalayil et al., 2021; Johnsson et al., 2022). They are often tissue-specific and correlate with pathologic processes, thus making them prime therapeutic targets. Furthermore, lncRNAs may directly interact with RNAs, DNAs, and proteins, thus exerting biological functions by acting as transcriptional regulators, miRNA sponges, molecular bait, or protein complex scaffolds (Huarte, 2015; Schmitt and Chang, 2016). LncRNAs may regulate gene expression via chromatin remodeling, epigenomic regulation, gene

* Corresponding authors.
E-mail addresses: leli@hainmc.edu.cn (L. Li), Yaohailan2020@163.com (H. Yao).
[1] These authors contribute equally to this work and should be considered co-first authors.

https://doi.org/10.1016/j.virusres.2023.199250
Received 14 July 2023; Received in revised form 8 October 2023; Accepted 18 October 2023

splicing, and transcriptional or posttranscriptional modulation (Cardenas-Diaz et al., 2019; Liang et al., 2022; Lin et al., 2021). Moreover, by functioning as miRNA sponges or competing endogenous RNAs (ceRNAs), lncRNAs have the potential to regulate vast networks of target genes (Xue et al., 2022). Several reports have demonstrated the functions of lncRNAs in viral response. For example, Ma et al. (2021) reported that lncRNAs play a critical role in replication and induce immune activation during the early HIV-1 infection process. Furthermore, Zhang et al. (2016) demonstrated that hepatocellular carcinomas with different viral etiologies have diverse lncRNA expression profiles, which has implications for disease-specific therapeutic interventions. Wang et al. (2020) also demonstrated that lncRNA-GM is altered during viral infection, participates in host metabolism and innate immunity, and impacts the viral evasion. Thus, there is a precedent for lncRNA involvement as a key mediator of viral response.

Our previous findings suggest that miRNA-21 is downregulated during CVB3 infection and mediates viral replication, leading to myocarditis (He et al., 2019). Therefore, lncRNAs upstream of miRNA-21 may function as ceRNAs and thus represent new molecular targets for the intervention of CVB3-associated myocarditis. Here, we demonstrate that CVB3 induces lncRNA-MEG3 expression and that MEG3 interacts with miRNA-21 to modulate CVB3 infection by targeting the P38 MAPK signaling pathway. Our results elucidate how CVB3 promotes its replication with functional outcomes and therapeutic potential.

2. Materials and methods

2.1. Virus and animals

The CVB3M strain was a gift from Yang at the University of British Columbia, Canada, and was pasaged in HeLa cells (Liu et al., 1999). The CVB3 sequence corresponds to accession number M33854.1 in the NCBI database. BALB/c male mice (6–8 weeks old) were purchased from the Institute of Laboratory Animal Sciences of China (Beijing, China).

2.2. Microarray analysis

For global profiling of human lncRNAs and protein-coding transcripts, we analyzed the hearts of three CVB3-infected and three control mice using ArrayStar mice Microarray V3.0. Sample processing and hybridization were performed according to the Agilent One-Color Microarray-Based Gene Expression Analysis protocol (Agilent Technology). Briefly, the rRNA was removed from 1 mg of total RNA (NEB NextrRNA Depletion Kit, USA). Then, each sample was amplified and transcribed into cRNA along the entire length of the transcripts without 3′ bias utilizing random primers. The Agilent Quick Amp Labeling kit was employed to normalize the values, and then LncRNAs and mRNAs for which at least one out of two groups had present or marginal flags were chosen for further data analysis. LncRNAs with $P < 0.05$ and foldchange >1.5 between samples were selected for hierarchical clustering. DIANA was used to predict miRNA-21-related LncRNAs, with the miTG-score set at 0.6, and the results were combined with the altered LncRNAs detected by microarray. Fold change was set at >1.5 and a significant difference at $P < 0.05$.

2.3. RNA extraction and quantitative real-time PCR

Total RNA from mouse tissues and cell lines was extracted using TRIzol reagent according to the manufacturer's protocol. The cytoplasmic fractions were extracted utilizing Cytoplasmic Extraction Reagents (Thermo Scientific, USA). For mRNA and miRNA, total RNA was processed using gDNA remover (TaKaRa, Japan), and cDNA was synthesized using a Reverse Transcription Kit (TaKaRa, Japan). MiRNA and LncRNA were quantified using SYBR Green Real-time PCR Master Mix (Life Technologies). GAPDH or U6 was utilized as an internal standard control. The relative RNA expression levels were calculated using the $2^{-\Delta\Delta CT}$ method. The specific primers used are listed in Additional File 1: Table 1.

2.4. Viral plaque assays and histological analysis of heart tissues

To detect the viral titers in HeLa cells, supernatants were collected at 6, 12, and 24 h post-infection, and the cell debris was discarded by centrifugation for 5 min at 2000 rpm. Lysates of infected cells were collected as previously described (He et al., 2019). To detect the viral loads of tissues, hearts from mice were weighed, homogenized in 0.5 ml MEM, and centrifuged at 1000 rpm for 10 min. The viral titers in the supernatants, cell lysates, and infected tissues were analyzed by viral plaque assay as previously described (He et al., 2015) and are expressed as PFU/ml and PFU/gram. To assess the severity of myocarditis, paraffin-embedded sections of heart tissues were stained with hematoxylin-eosin and examined histopathologically for evidence of inflammation and necrosis.

2.5. Adeno-associated virus generation and in vivo infection

For LncRNA-MEG3 knockdown, adeno-associated vectors (AAV9) were used to construct short hairpin RNAs (shRNAs) targeting MEG3 (AAV-MEG3) or a non-specific control (AAV-CON). Oligonucleotides targeting MEG3 (5′-GCGUCUUCCUGUGCCAUUU-3′) were synthesized based on the sequence of mouse MEG3 (NR_003633). The viruses were generated using the AAV Helper-Free System, with pAAV-RC plasmid and pHelper plasmid (GeneChem Co. Ltd. Shanghai, China). Viral titers were evaluated as described previously (Yu et al., 2008).

For infection, 2×10^{11} transduction units of AAV-MEG3 or AAV-CON were intravenously injected into each mouse via the caudal vein. The mice were then inoculated intraperitoneally with 1×10^5 plaque-forming units (PFU, LD50) of CVB3 virus per mouse for 10 d. A subset of the mice ($n = 15$ per group) was monitored daily for survival, and another subset ($n = 10$ per group) was euthanized on d 3, 5, or 7 after infection with CVB3 for experimental evaluation. Survival was monitored over a 22-d time course. Experiments were carried out 3 times, and representative results are shown.

2.6. Luciferase reporter assays

MEG3-WT/Mut reporters were constructed by subcloning wild-type (WT) or mutant (Mut) sequences of MEG3 complementary to miRNA-21 into the pmirGLO dual-luciferase vector. Then, these reporters

Table 1
Primers used in this study.

Primer	Sequence
Reverse transcription primer for miRNA-21	5′ CTCAACTGGTGTCGTGGAGTCGGCAATTCAGTTGAGTCAACA 3′
Sense primer for miRNA-21	5′-ACACTCCAGCTGGCTAGCTTATCAGACTGATG-3′
Anti-sense primer for miRNA-21	5′-CTCAACTGGTGTCGTGGA-3′
Sense primer for MEG3	5′-ATCATCCGTCCACCTCCTTGTCTTC-3′
Anti-sense primer for MEG3	5′-GTATGAGCATAGCAAAGGTCAGGGC-3′
Sense primer for CREB5	5′-CCCTGCCCAACCCTACAATG-3′
Anti-sense primer for CREB5	5′-GGACCTTGCATCCCCATGAT-3′
Sense primer for GAPDH	5′-AATGCCTCCTGCACCACCAAC-3′
Anti-sense primer for GAPDH	5′-AAGGCCATGCCAGTGAGCTTC-3′

were co-transfected with miRNA-21 mimics or NC mimics into 293T cells. After 2 d, the Dual-Luciferase Report Assay System (Promega) was used to measure luciferase activity. Relative luciferase activity was defined as the ratio of the relative light unit of firefly luciferase to that of Renilla luciferase.

2.7. MS2-RIP

We used the MS2-RIP method to detect the interaction of LncRNA-MEG3 and miRNA-21 (Yoon et al., 2012). Briefly, pcDNA3.1-MS2, pcDNA3.1-MS2-MEG3, and pcDNA3.1-MS2-MEG3-MUT were constructed and co-transfected along with pGST-MS2 into HeLa cells using Lipofectamine3000 reagent (Invitrogen, USA). After 48 h, the cells were collected and lysed to perform RNA immunoprecipitation (RIP) experiments using GST-Sepharose beads (Thermo Scientific, USA). Finally, purified RNAs were isolated and identified by real-time PCR to confirm the presence of binding targets. The primers used for detecting miRNA-21 are shown in Table 1.

2.8. Protein detection

HeLa cells or homogenated mouse heart tissues were collected at the indicated time points and were lysed in RIPA buffer (Kangwei, Beijing, China). Antibodies for detecting MAP2K3, P38 MAPK, P-P38 MAPK, HSP 27, P-HSP 27, and GAPDH were purchased from Cell Signaling Technology (Cell Signaling Technology, Inc, China). Western blotting was conducted as described previously (He et al., 2019).

2.9. Cell viability assays

According to the manufacturer's instructions, cell viability was measured using an MTS assay kit (Promega, Madison). HeLa cells were transduced with siRNA-MEG3 and infected with CVB3 at MOI=1. After 24 h, the cells were incubated with MTS solution for 2 h, and the absorbance was measured at 492 nm using a microplate reader. The viability of the control cells was defined as 100 %, and the viability of infected cells was expressed as a ratio of the absorbance of the infected cells to that of the control cells.

2.10. Statistical analysis

All statistical analyses were performed using the SPSS 16.0 computer software program (SPSS, Inc., Chicago, IL). Survival was analyzed using the log-rank (Mantel-Cox) method. The significance of variability among the experimental groups was determined by the Mann-Whitney U test. All differences were considered statistically significant at $P < 0.05$.

3. Results

3.1. LncRNA-MEG3 expression is elevated post CVB3 infection

To obtain a lncRNA expression profile of the CVB3 infection process, we performed a lncRNA microarray utilizing a mouse model on d 5 after CVB3 infection at PFU 1*10E5(LD50), which correlates with the acute infection stage. Results from 3 control mice (N-1, N-2, and N-3) and 3

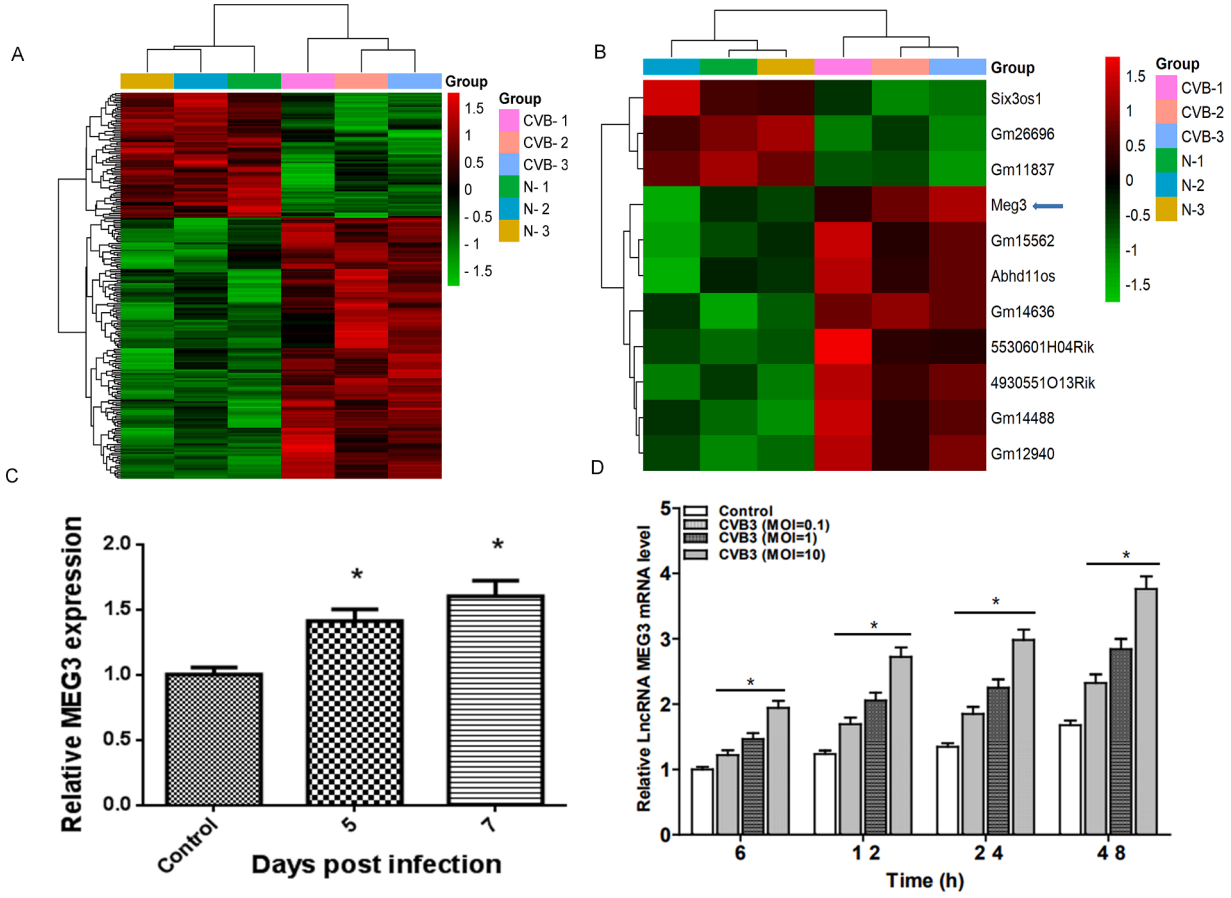

Fig. 1. LncRNA MEG3 is upregulated post CVB3 infection. (A) Heat map and hierarchical clustering of lncRNA expression in the heart of uninfected mice (N-1, N-2, N-3) and CVB3-infected mice (CVB-1, CVB-2, CVB-3) at 5 d post-infection (fold-change ≥1.5, $P < 0.05$, $n = 3$ per group). (B) Heatmap and hierarchical clustering of altered lncRNAs from panel A that are predicted bioinformatically to interact with miRNA-21 (fold change>1.5, $P < 0.05$). (C) LncRNA-MEG3 expression was detected by real-time PCR of mouse hearts before infection and at 5 and 7 d post CVB3 infection. (D) LncRNA-MEG3 expression was detected by real-time PCR of HeLa cells at different time points and multiplicities of infection (MOI) of CVB3 infection. * represents $P < 0.05$.

infected mice (CVB-1, CVB-2, and CVB-3) showed that 268 lncRNAs were differently expressed, with 183 increased and 85 decreased in the CVB3 infected group [absolute fold-change ≥1.5, $P < 0.05$] (Fig. 1A). Because one of the main functions of lncRNAs involves acting as competing endogenous RNAs (ceRNAs) for miRNAs, and we previously demonstrated that miRNA-21 is altered post CVB3 infection (He et al., 2019), we used DIANA and miRanda tools to predict potential lncRNAs that may directly interact with miRNA-21. We then intersected the two data sets and identified 11 candidate lncRNAs that were predicted to be miRNA-21-associated and were also upregulated by CVB3 infection (Fig. 1B) (fold change >1.5, $P < 0.05$). Among the 11 lncRNAs, we selected MEG3 for subsequent analysis because it has been demonstrated to be dysregulated in response to other viruses and to be associated with cardiac hypertrophy, cardiac fibrosis, and ischemic injury (Li et al., 2022; Piccoli et al., 2017; Sethuraman et al., 2017; Tao et al., 2018; Xiang et al., 2020; Zhang et al., 2019). Real-time PCR analysis verified that lncRNA-MEG3 expression was upregulated at 5 and 7 d post CVB3 infection in mouse hearts ($n = 6$, Fig. 1C). Because ceRNAs function in the cytoplasm, we infected HeLa cells with different MOIs and evaluated MEG3 expression in the cytoplasm. The results verify that MEG3 was highly expressed in the HeLa cytoplasm and that expression increased over 48 h post-infection, with the expression elevated with increasing CVB3 MOI (Fig. 1D). Thus, these results suggest that MEG3 is a CVB3-induced lncRNA that may interact with miRNA-21.

3.2. LncRNA-MEG3 functions as a sponge for miRNA-21

To verify the potential role of MEG3 in modifying miRNA-21 expression, we subcloned the full-length lncRNA-MEG3 (MEG3 WT) and a mutant within the "seed sequence" that is predicted to ablate miRNA-21 binding (MEG3 MUT) into a pmirGLO dual luciferase reporter vector (Fig. 2A). These constructed reporters were co-transfected with miRNA-21 or control (NC) mimics into 293T cells. Dual luciferase assays showed that miRNA-21 mimics, but not NC mimics, suppress the luciferase activity of MEG3 WT but not MEG MUT (Fig. 2B), indicating that a sequence-specific interaction may exist between lncRNA-MEG3 and miRNA-21.

To directly determine whether MEG3 binds to endogenous miRNA-21, we performed MS2-RIP pulldown assays. The miRNA-21 levels in the MS2-GST complex were higher in the MEG3 WT group than the MEG3 MUT group, suggesting that MEG3 was significantly associated with miRNA-21 (Fig. 2C). Thus, these results further support an endogenous interaction between lncRNA MEG3 and miRNA-21.

3.3. Inhibition of lncRNA-MEG3 alleviates CVB3 replication by modulating the miRNA-21-mediated P38-MAPK signaling pathway

We previously demonstrated that exogenous expression of miRNA-21 inhibits CVB3 replication (He et al., 2019). We, therefore, evaluated the function of lncRNA-MEG3 in the CVB3 replication process. To this end, we synthesized a siRNA specifically targeting MEG3. Our results demonstrated that MEG3 knockdown led to increased expression of miRNA-21, thus further supporting a function for MEG3 as a miRNA-21 sponge (Fig. 3A and B). Next, we infected HeLa cells with CVB3 at MOI = 1 and evaluated the number of viral plaques 12 h later. There were significantly fewer plaques in siRNA-MEG3 cells than in siRNA-Control cells (Fig. 3C), supporting a role for MEG3 in promoting CVB3 replication by sponging miRNA-21. As our previous study also demonstrated that miRNA-21 inhibits CVB3 replication by inhibiting MAP2K3 and the P38 MAPK signaling pathway (He et al., 2019), we detected MAP2K3, P-P38 MAPK, and P-HSP27 levels in CVB3-infected MEG3 knockdown cells and found that they were all reduced, while total P38 MAPK and HSP27 were not altered by siRNA-MEG3. These results suggest that MEG3 regulates the P-P38 MAPK pathway activation to modulate the CVB3 replication process (Fig. 3D). To evaluate whether these signaling changes may mediate effects on cell viability, we performed proliferation assays. Significantly enhanced proliferation rates were observed in MEG3 siRNA-transfected cells (Fig. 3E), which is consistent with a role for MEG3 in mediating CVB3-associated cytotoxicity.

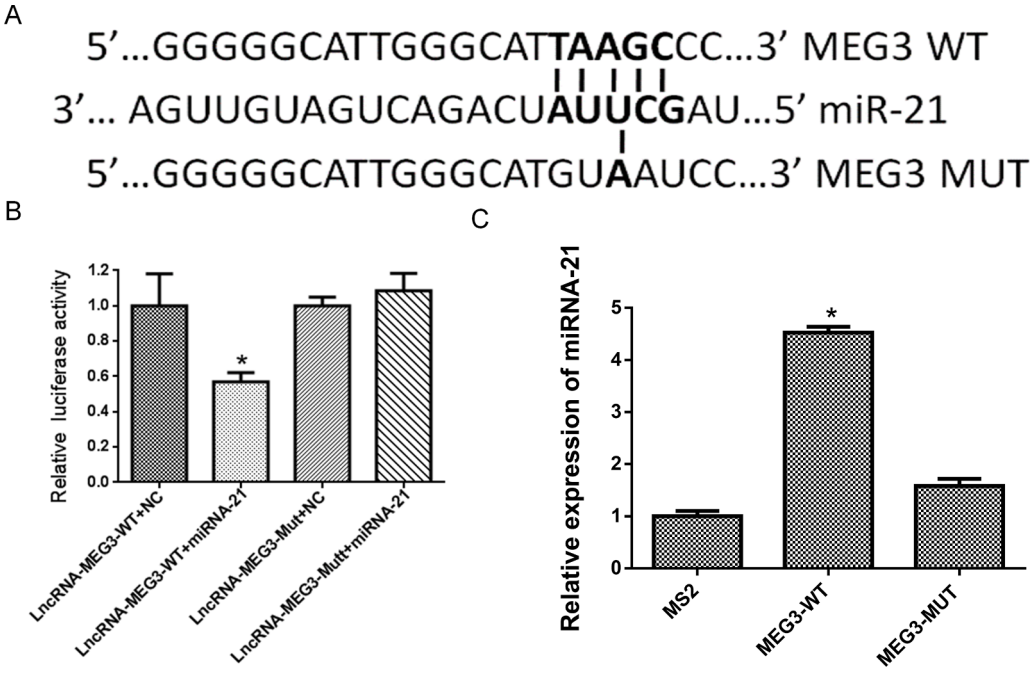

Fig. 2. LncRNA-MEG3 functions as a sponge for miRNA-21. (A) Sequence alignment of miRNA-21 with a putative binding site within the wild-type LncRNA-MEG3 (MEG3 WT) and a mutated sequence (MEG3 MUT) that was generated as a control. (B) Dual luciferase assays were conducted to verify the role of MEG3 in modifying miRNA-21. MEG3 WT and MEG3 MUT dual-luciferase reporters were co-transfected with miRNA-21 or a control miRNA (NC) into 293T cells, and the luciferase activity was detected. (C) MS2-RIP assays were conducted to detect the interaction of miRNA-21 with co-expressed MEG3-WT versus MEG3-MUT directly. The MS2 sample (miRNA-21 expression without co-expressed MEG3) was included as an additional control. * represents $P < 0.05$.

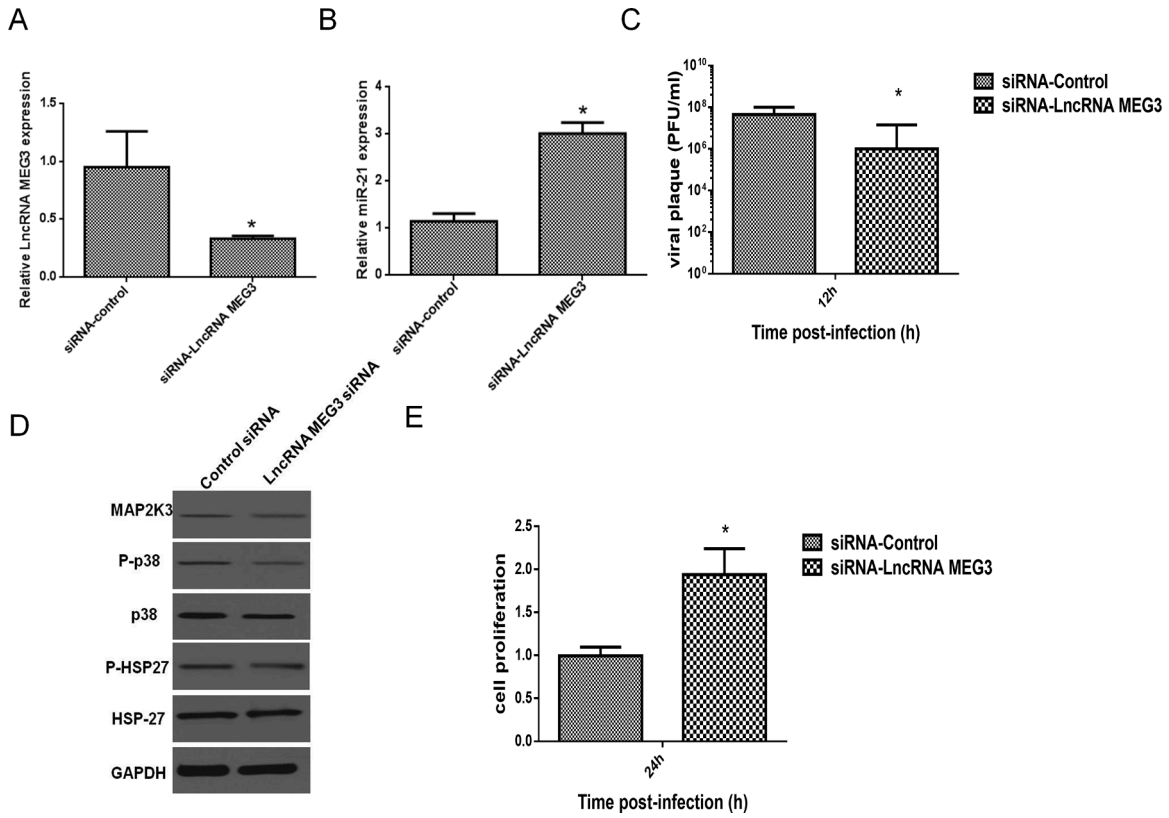

Fig. 3. LncRNA-MEG3 knockdown inhibits CVB3 replication in HeLa cells by increasing miRNA-21 and reducing P38 MAPK activation. HeLa cells were transfected with siRNA-MEG3 or control siRNA plasmids and then were infected 24 h later with CVB3 at MOI=1. (A) RT-PCR of MEG3 expression at 24 h post-transfection of siRNA-MEG3 and siRNA-control plasmids to verify knockdown efficacy. (B) miRNA-21 expression in HeLa cells was detected at 24 h post-transfection. (C) Viral replication in HeLa cell supernatants was detected by plaque formation assay after transfection of siRNA-MEG3 and siRNA control plasmids, followed by CVB3 infection for 12 h. (D) Western blotting was conducted to detect MAP2K3 and total and phosphorylated (activated) P38 and downstream HSP27 levels in HeLa cells transfected with siRNA-MEG3 and siRNA control plasmids followed by CVB3 infection for 12 h. GAPDH was evaluated as a control. (E) HeLa cell viability was detected by MTS assay 24 h post-CVB3 infection. Representative results from 3 independent experiments are shown. * represents $P < 0.05$.

To determine whether MEG3 knockdown may also reduce CVB3 pathogenesis in a mouse model of viral myocarditis, we constructed an adeno-associated virus (AAV) vector containing MEG3-shRNA and injected 2×10^{11} transduction units of AAV-shMEG3 or AAV-Control via the caudal vein before CVB3 infection. MEG3 expression was confirmed to be dramatically inhibited at 3–7 d in the hearts of mice that were infected with AAV-shMEG3+ CVB3 (Fig. 4A), and in turn, miRNA-21 expression was increased (Fig. 4B). Next, we inoculated 1×10^5 pfu (LD50) of CVB3 intraperitoneally into mice after infection with shMEG or Control AAV. The CVB3 titers were significantly suppressed at 3–7 d post-infection in the AAV-MEG3 group as compared to the control group at each of the time points tested (Fig. 4C), which is consistent with the inhibition by MEG3 of viral replication both *in vitro* and *in vivo*. We further analyzed MAP2K3, P-P38/total P38, and P-HSP27/total HSP27 protein levels at 3 d post-infection, which suggested that MAPK pathway activation was reduced in the hearts of mice with MEG3 knockdown (Fig. 4D). These results suggest that inhibition of MEG3 may alleviate the CVB3 replication process by targeting the P38 MAPK pathway, which may be mediated through upregulated miRNA-21 expression. To determine the physiological outcome of MEG3 inhibition in CVB3-infected mice, we examined the histopathology of infected mouse hearts. Mice in the control group showed significant necrosis and signs of mononuclear cell infiltration on d 7 post-infection, while the mice with reduced MEG3 showed only minor dropsy and hemorrhage (Fig. 4E). Furthermore, the survival rate was improved in MEG3-knockdown mice after CVB3 infection (Fig. 4F), thus indicating a protective function of lncRNA MEG3 knockdown.

3.4. LncRNA-MEG3 is modulated by CREB5 in the CVB3 infection process

To evaluate regulatory processes upstream of MEG3, we used JASPAR (https://jaspar.genereg.net) to screen the promoter sequence 3000 bp 3′ of the LncRNA MEG3 coding site and predict transcription factors that may bind and modulate its expression. Putative MEG3 promoter-binding transcription factors were evaluated by microarray analysis for upregulation post CVB3 infection in the mouse heart, and 12 candidate regulators of MEG3 expression in CVB3-infected cells were identified (Table 2). The upregulation of ten of these 12 transcription factors post-infection was validated by real-time PCR (Fig. 5A). Previous studies have reported that cAMP response element-binding protein (CREB) binds to the MEG3 promoter and modulates its expression (Zhang et al., 2017) and that the CREB/p38 MAPK signaling axis regulates a variety of important physiological processes (Koga et al., 2019; Lonze et al., 2002; Zhang et al., 2017; Zhu et al., 2019); thus, we evaluated the effect of CREB5 knockdown on MEG3 expression in HeLa cells. The results verify that MEG3 levels were decreased in the siRNA-CREB5 treatment group (Fig. 5B). We next infected CVB3 at MOI = 1 and detected the effect of siRNA-CREB5 on viral plaque formation. The viral levels in the cell supernatant were significantly reduced at 48 h post-infection in CREB5 knockdown cells (Fig. 5C). Thus, inhibition of CREB5 reduces CVB3 replication by inhibiting MEG3, indicating that CREB5 could potentially serve as a mediator of the MEG3-miRNA21-P38 MAPK axis in CVB3-infected mouse hearts (Fig. 6).

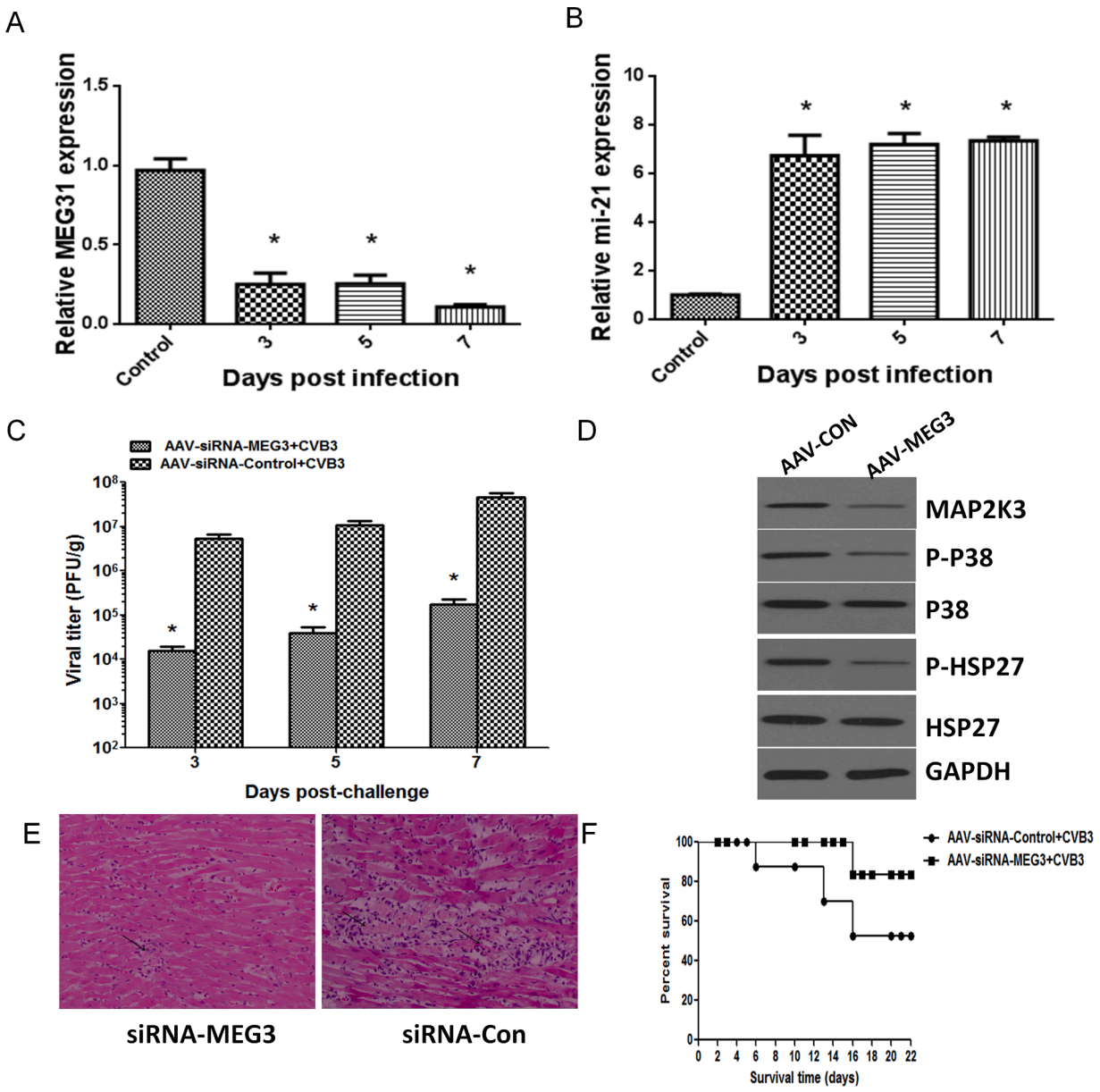

Fig. 4. MEG3 knockdown alleviates CVB3 pathogenesis in mice. 2 × 10^{11} transduction units of adeno-associated virus (AAV) containing MEG3-shRNA or a control (AAV-CON) were intravenously injected into mice via the caudal vein. The mice were then inoculated intraperitoneally with 1 × 10^5 plaque-forming units (PFU, LD50) of CVB3 virus. (A) MEG3 expression in the heart was evaluated over time to verify the efficacy of knockdown in AAV-MEG-shRNA and CVB3-infected mice. (B) The relative miRNA-21 expression in mouse hearts was determined at the same time points as in panel A ($n = 5$). (C) CVB3 viral titers were detected by viral plaque assay of heart tissue homogenates from mice at the indicated time after infection with AAV-MEG3-shRNA or AAV-CON followed by CVB3 ($n = 5$). (D) Western blotting of MAP2K3, P-P38 MAPK, and P-HSP 27 expression in the hearts of mice 3 d after infection with AAV-CON or AAV-MEG3-shRNA followed by CVB3. GAPDH was evaluated as a control. Representative results from 3 independent experiments are shown. (E) Histological analysis of heart tissues at d 7 post-infection for mice infected with AAV-MEG3-shRNA or AAV-CON followed by CVB3. Examples of necrosis and calcification are shown (black arrow). Original magnification, × 200. (F) Survival curves showing the antiviral effects of AAV-MEG3-shRNA on mouse survival. Mice were pretreated with AAV-MEG3-shRNA or AAV-CON followed by infection of LD50 CVB3, and survival was evaluated over 22 d ($n = 15$). Results are representative of 3 independent experiments.

4. Discussion

LncRNAs in the cytoplasm serve as "miRNA sponges" that reverse the negative effects of miRNAs on their target genes (Cheng et al., 2020; Saltarella et al., 2022). Our previous results indicate that CVB3, an important pathogenic agent of viral myocarditis, pancreatitis, and cerebritis, alters miRNA-21 expression and that exogenous expression of miRNA-21 inhibits CVB3 release by targeting the P38 MAPK signaling pathway (He et al., 2019), though lncRNAs that function within a CVB3-regulated lncRNA/miRNA-21 axis were uncharacterized. In this study, we evaluated the lncRNA expression profile in a CVB3-induced viral myocarditis mouse model and used bioinformatics analysis to identify candidate lncRNAs that may function upstream of miRNA-21. Our results suggest that lncRNA-MEG3 is upregulated in the cytoplasm of HeLa cells post CVB3 infection and can sponge miRNA-21. The human lncRNA-MEG3 has 16 transcript variants (3 in mice), and transcript 1 has been widely studied for its ability to interact with miRNAs (Du et al., 2020; Su et al., 2015; Zhang et al., 2017). In this study, we designed amplifying primers according to lncRNA-MEG3 transcript variant 1, which is predicted to interact with miRNA-21. To validate the interaction between lncRNA-MEG3 and miRNA-21, we performed dual luciferase and RIP assays, and these results provide additional support for

Table 2
Upregulated transcription factors post CVB3 infection that were predicted to bind and regulate lncRNA-MEG3 expression. Bioinformatic prediction was conducted with JASPAR, and the results were compared with the altered transcription factors post-CVB3 infection identified by microarray. 12 possible transcription factors were found.

Gene	Regulation ([CVB3] vs. [N])	UniGene
Esrrb	Up	Mm.235550
Myc	Up	Mm.2444
Sox17	Up	Mm.279103
Hoxd9	Up	Mm.26544
Sox5	Up	Mm.1752
Creb5	Up	Mm.321138
Lhx4	Up	Mm.103624
Arid5a	Up	Mm.34316
Npas2	Up	Mm.2380
Arnt	Up	Mm.250265
Arntl	Up	Mm.440371
Atf3	Up	Mm.2706

their functional association within a CVB3-regulated axis. As additional evidence, lncRNA-MEG3 knockdown directly modulated miRNA-21 expression post-infection, reduced viral plaque levels, and increased cellular proliferation levels, thus providing a pathway in which lncRNA-MEG3 will likely play a key role. These results are significant in providing mechanistic insight into the signaling processes that underlie a devastating childhood infection and in identifying a potential therapeutic target that could be deployable as new noncoding RNA therapeutic technologies options emerge (Winkle et al., 2021).

This study further extends our previous results by demonstrating that miRNA-21 modulates p38 MAPK activation and that overexpression of miRNA-21 inhibits CVB3 replication by targeting the p38 MAPK family (He et al., 2019). Using specific siRNA-MEG3 24 h before CVB3 infection, we found that P-P38 MAPK and P-HSP27 in the P38 MAPK signaling pathway were reduced, correlated with the inhibition of CVB3 replication and increased cell proliferation. These results are consistent with an inhibitory role for p38 MAPK downstream of LncRNA-MEG3 promoted by CVB3 infection. Furthermore, our *in vitro* findings were verified in a mouse model, demonstrating that siRNA-MEG3 reduces p-P38 levels, improves heart tissue morphology, and extends survival rates after CVB3 infection in mice. Notably, the activation of the p38 MAPK pathway has been shown to underlie the apoptosis and necrosis of cardiomyocytes (Jensen et al., 2013), inflammation, and the release of inflammatory cytokines (Wu et al., 2015; Zheng et al., 2019), and increased collagen production that leads to CVB3-induced myocardial fibrosis (Jiang et al., 2016).

To further explore the upstream mechanisms by which CVB3 activates MEG3, we screened for transcription factors that may bind to and function within the sequence 3000 bp upstream of the MEG3 coding site. By combining bioinformatic prediction and microarray data, we identified 12 putative transcription factors and finally selected CREB5 as a candidate CVB-induced MEG3 transcription factor based on its established role in a variety of effectual biological processes (Koga et al., 2019). The CREB (cAMP response element-binding) proteins selectively activate numerous downstream genes through interactions with different partners and play a key role in promoting gluconeogenic (Zhu et al., 2019), fibrotic and cirrhotic livers (Zhang et al., 2017), as well as neuronal survival (Lonze et al., 2002). Recently, accumulating evidence has implied that CREB directly binds to the MEG3 proximal promoter region, which is critical for the promoter activity of MEG3 (Zhang et al., 2017). Consistently, our data demonstrate that the knockdown of CREB5 inhibits endogenous lncRNA-MEG3 expression and CVB3 viral plaque levels. Therefore, our results support a potential role of CREB5 in the lncRNA MEG3/miRNA-21/P38MAPK axis, which underlies the CVB3 replication process. Based on our findings, CREB5 may represent an additional potential target for inhibiting MEG3 to alleviate the effects of viral infection, suggesting a new theoretical approach for therapeutic

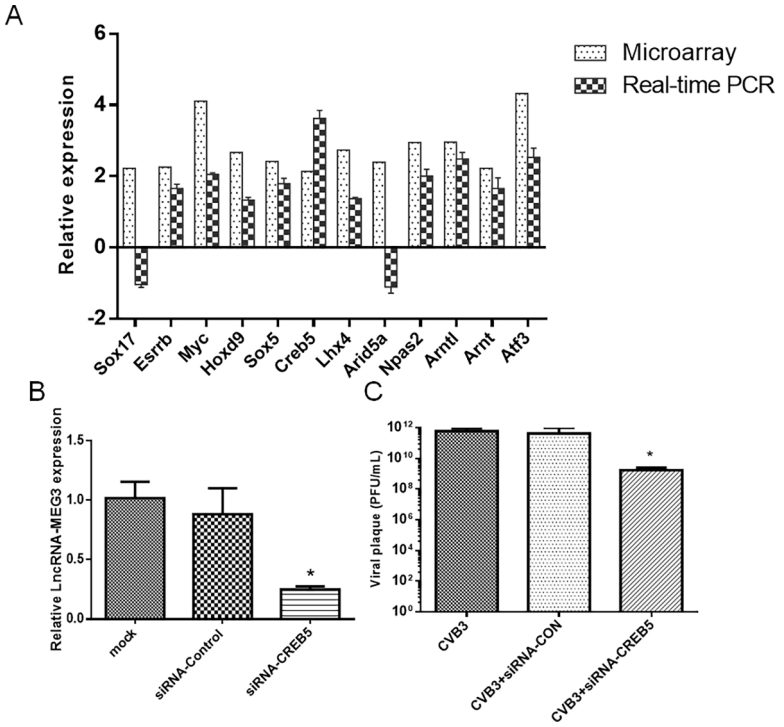

Fig. 5. LncRNA-MEG3 is regulated by CREB5 in the CVB3 infection response. (A) Real-time PCR was performed for 12 transcription factors that were predicted to bind the LncRNA-MEG3 promoter and were determined to be upregulated by CVB3 in microarray analysis of infected versus uninfected mouse hearts. Relative expression values are shown for microarray and real-time PCR. (B) HeLa cells were treated with a control or siRNA-CREB5 and infected with CVB3 at MOI=1 48 h later. LncRNA-MEG3 expression levels were detected by real-time PCR 24 h post-infection. (C) Viral replication was detected in supernatants 24 h post-infection by plaque assay. Results represent the average of triplicates and were repeated three times.

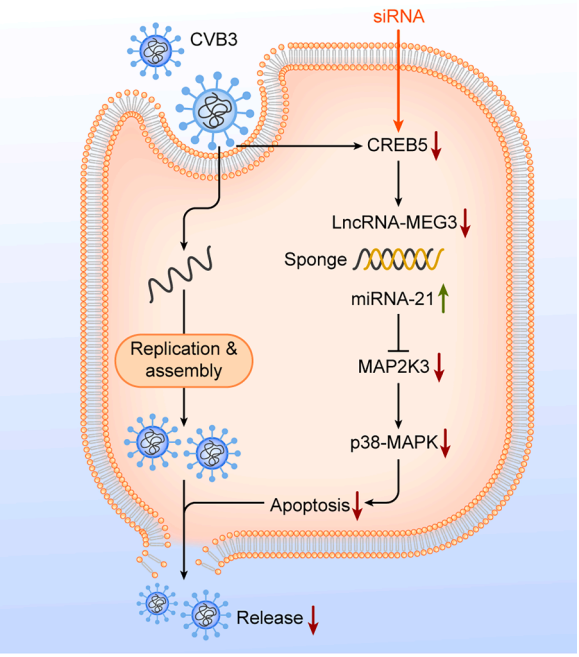

Fig. 6. Schematic depicting the molecular pathway involved in CVB3 replication and the mechanism underlying the inhibition of viral release by siRNA-CREB5. CVB3 infection reduces miRNA-21 levels through CREB5 and lncRNA MEG3, leading to activation of the p38-MAPK pathway, apoptosis of the host cell, and viral release. Inhibiting CREB5 with siRNA increases the levels of miRNA-21, which inhibits the p38-MAPK pathway and ultimately leads to reduced viral release. The up and down arrows beside the molecules and processes indicate promotion and inhibition following siRNA treatment.

intervention.

As a limitation of this work, MEG3 was one of 11 candidate lncRNAs, and CREB5 was one of 12 candidate transcriptional activators associated with CVB3-induced mi-RNA21 expression. Furthermore, evidence has shown that the p38 MAPK and CREB pathways can cross-regulate each other (Koga et al., 2019), indicating that the MEG3-miRNA21-p38 MAPK axis described in this study may function within a complex network of inter-related regulatory pathways. Future studies to verify the contribution of CREB5 in the mouse heart and to extend the MEG3/miRNA-21/P38MAPK axis to include additional contributing regulators would help to provide a more comprehensive understanding of mechanisms and potential therapeutic targets to alleviate the outcome of CVB3 infections.

Funding information

This study was funded by NHC Key Laboratory of Tropical Disease Control, Hainan Medical University, Haikou, Hainan, China, (2022NHCTDCKFKT11002), Public service development and reform pilot project of Beijing Medical Research Institute (BMR2021-3), National Natural Science Foundation of China (31800153), Research Foundation of Capital Institute of Pediatrics (JCYJ-2023-01), Clinical Testing research fund of the Capital Institute of Pediatrics CTR-2023-001, CTR-2023-003.

Declarations of ethics statement

The animal study was approved by the Review Board of the Capital Institute of Pediatrics with the permit number KSDWLL2017009 (Beijing, China).

CRediT authorship contribution statement

Feng He: Investigation, Writing – original draft, Writing – review & editing. **Zhuo Liu:** Investigation, Writing – original draft, Formal analysis, Writing – review & editing. **Miao Feng:** Methodology, Writing – review & editing. **Zonghui Xiao:** Methodology, Writing – review & editing. **Xiaoyu Yi:** Methodology, Writing – review & editing. **Jianxin Wu:** Formal analysis, Writing – review & editing. **Zhewei Liu:** Formal analysis, Writing – review & editing. **Gaoyu Wang:** Formal analysis, Writing – review & editing. **Le Li:** Visualization, Writing – review & editing. **Hailan Yao:** Visualization, Writing – review & editing.

Declaration of Competing Interest

All authors declare that they have no competing interests.

Data availability

Data will be made available on request.

Acknowledgments

The authors acknowledge the help of Jizhen Zou, Ping Xiao, and Dan Liu in the Department of Pathology at the Capital Institute of Pediatrics (Beijing, China) for technical support.

References

Aryankalayil, M.J., Martello, S., Bylicky, M.A., Chopra, S., May, J.M., Shankardass, A., MacMillan, L., Sun, L., Sanjak, J., Vanpouille-Box, C., Eke, I., Coleman, C.N., 2021. Analysis of lncRNA-miRNA-mRNA expression pattern in heart tissue after total body radiation in a mouse model. J. Transl. Med. 19, 336.

Ballinger, M.J., Christian, R.C., Moore, L.D., Taylor, D.J., Sabet, A., 2022. Evolution and diversity of inherited viruses in the nearctic phantom midge, Chaoborus americanus. Virus Evol. 8, veac018.

Cardenas-Diaz, F.L., Osorio-Quintero, C., Diaz-Miranda, M.A., Kishore, S., Leavens, K., Jobaliya, C., Stanescu, D., Ortiz-Gonzalez, X., Yoon, C., Chen, C.S., Haliyur, R., Brissova, M., Powers, A.C., French, D.L., Gadue, P., 2019. Modeling monogenic diabetes using human ESCs reveals developmental and metabolic deficiencies caused by mutations in HNF1A. Cell Stem Cell 25, 273–289 e275.

Cheng, L., Nan, C., Kang, L., Zhang, N., Liu, S., Chen, H., Hong, C., Chen, Y., Liang, Z., Liu, X., 2020. Whole blood transcriptomic investigation identifies long non-coding RNAs as regulators in sepsis. J. Transl. Med. 18, 217.

Du, X., Tian, D., Wei, J., Yan, C., Hu, P., Wu, X., Yang, W., 2020. MEG3 alleviated LPS-induced intestinal injury in sepsis by modulating miR-129-5p and surfactant protein D. Mediat. Inflamm. 2020, 8232734.

He, F., Xiao, Z., Yao, H., Li, S., Feng, M., Wang, W., Liu, Z., Liu, Z., Wu, J., 2019. The protective role of microRNA-21 against coxsackievirus B3 infection through targeting the MAP2K3/P38 MAPK signaling pathway. J. Transl. Med. 17, 335.

He, F., Yao, H., Wang, J., Xiao, Z., Xin, L., Liu, Z., Ma, X., Sun, J., Jin, Q., Liu, Z., 2015. Coxsackievirus B3 engineered to contain microRNA targets for muscle-specific microRNAs displays attenuated cardiotropic virulence in mice. J. Virol. 89, 908–916.

Huarte, M., 2015. The emerging role of lncRNAs in cancer. Nat. Med. 21, 1253–1261.

Jensen, K.J., Garmaroudi, F.S., Zhang, J., Lin, J., Boroomand, S., Zhang, M., Luo, Z., Yang, D., Luo, H., McManus, B.M., Janes, K.A., 2013. An ERK-p38 subnetwork coordinates host cell apoptosis and necrosis during coxsackievirus B3 infection. Cell Host Microbe 13, 67–76.

Jiang, S., Jiang, D., Zhao, P., He, X., Tian, S., Wu, X., Tao, Y., 2016. Activation of AMP-activated protein kinase reduces collagen production via p38 MAPK in cardiac fibroblasts induced by coxsackievirus B3. Mol. Med. Rep. 14, 989–994.

Johnsson, P., Ziegenhain, C., Hartmanis, L., Hendriks, G.J., Hagemann-Jensen, M., Reinius, B., Sandberg, R., 2022. Transcriptional kinetics and molecular functions of long noncoding RNAs. Nat. Genet. 54, 306–317.

Kaplan, M.H., Klein, S.W., McPhee, J., Harper, R.G., 1983. Group B coxsackievirus infections in infants younger than three months of age: a serious childhood illness. Clin. Infect. Dis. 5, 1019–1032.

Kim, K.S., Hufnagel, G., Chapman, N.M., Tracy, S., 2001. The group B coxsackieviruses and myocarditis. Rev. Med. Virol. 11, 355–368.

Koga, Y., Tsurumaki, H., Aoki-Saito, H., Sato, M., Yatomi, M., Takehara, K., Hisada, T., 2019. Roles of cyclic AMP response element binding activation in the ERK1/2 and p38 MAPK signalling pathway in central nervous system, cardiovascular system, osteoclast differentiation and mucin and cytokine production. Int. J. Mol. Sci. 20, 1346.

Lai, C., Liu, L., Liu, Q., Wang, K., Cheng, S., Zhao, L., Xia, M., Wang, C., Duan, Y., Zhang, L., Liu, Z., Luo, J., Wang, X., Chen, R., Yang, P., 2021. Long noncoding RNA

AVAN promotes antiviral innate immunity by interacting with TRIM25 and enhancing the transcription of FOXO3a. Cell Death Differ. 28, 2900–2915.
Li, Z., Gao, J., Sun, D., Jiao, Q., Ma, J., Cui, W., Lou, Y., Xu, F., Li, S., Li, H., 2022. LncRNA MEG3: potential stock for precision treatment of cardiovascular diseases. Front. Pharmacol. 13, 1045501.
Liang, J., Liu, C., Xu, D., Xie, K., Li, A., 2022. LncRNA NEAT1 facilitates glioma progression via stabilizing PGK1. J. Transl. Med. 20, 80.
Lin, H., Zhu, Y., Zheng, C., Hu, D., Ma, S., Chen, L., Wang, Q., Chen, Z., Xie, J., Yan, Y., Huang, X., Liao, W., Kitakaze, M., Bin, J., Liao, Y., 2021. Antihypertrophic Memory After Regression of Exercise-Induced Physiological Myocardial Hypertrophy Is Mediated by the Long Noncoding RNA Mhrt779. Circulation 143, 2277–2292.
Liu, Z., Carthy, C.M., Cheung, P., Bohunek, L., Wilson, J.E., McManus, B.M., Yang, D., 1999. Structural and functional analysis of the 5′ untranslated region of coxsackievirus B3 RNA: *in vivo* translational and infectivity studies of full-length mutants. Virology 265, 206–217.
Lonze, B.E., Riccio, A., Cohen, S., Ginty, D.D., 2002. Apoptosis, axonal growth defects, and degeneration of peripheral neurons in mice lacking CREB. Neuron 34, 371–385.
Ma, L., Zhang, H., Zhang, Y., Li, H., An, M., Zhao, B., Ding, H., Xu, J., Shang, H., Han, X., 2021. Integrated analysis of lncRNA, miRNA and mRNA profiles reveals potential lncRNA functions during early HIV infection. J. Transl. Med. 19, 135.
Ozsvár, Z., Deák, J., Pap, A., 1992. Possible role of Coxsackie-B virus infection in pancreatitis. Int. J. Pancreatol. 11, 105–108.
Piccoli, M.T., Gupta, S.K., Viereck, J., Foinquinos, A., Samolovac, S., Kramer, F.L., Garg, A., Remke, J., Zimmer, K., Batkai, S., Thum, T., 2017. Inhibition of the cardiac fibroblast–enriched lncRNA Meg3 prevents cardiac fibrosis and diastolic dysfunction. Circ. Res. 121, 575–583.
Rassmann, A., Martin, U., Saluz, H.P., Peter, S., Munder, T., Henke, A., 2013. Identification of gene expression profiles in HeLa cells and HepG2 cells infected with Coxsackievirus B3. J. Virol. Methods 187, 190–194.
Rorabaugh, M.L., Berlin, L.E., Heldrich, F., Roberts, K., Rosenberg, L.A., Doran, T., Modlin, J.F., 1993. Aseptic meningitis in infants younger than 2 years of age: acute illness and neurologic complications. Pediatrics 92, 206–211.
Saltarella, I., Lamanuzzi, A., Desantis, V., Di Marzo, L., Melaccio, A., Curci, P., Annese, T., Nico, B., Solimando, A.G., Bartoli, G., Tolomeo, D., Storlazzi, C.T., Mariggio, M.A., Ria, R., Musto, P., Vacca, A., Frassanito, M.A., 2022. Myeloma cells regulate miRNA transfer from fibroblast-derived exosomes by expression of lncRNAs. J. Pathol. 256, 402–413.
Schmitt, A.M., Chang, H.Y., 2016. Long noncoding RNAs in cancer pathways. Cancer Cell 29, 452–463.
Sethuraman, S., Gay, L.A., Jain, V., Haecker, I., Renne, R., 2017. microRNA dependent and independent deregulation of long non-coding RNAs by an oncogenic herpesvirus. PLoS Pathog. 13, e1006508.
Su, W., Xie, W., Shang, Q., Su, B., 2015. The long noncoding RNA MEG3 is downregulated and inversely associated with VEGF levels in osteoarthritis. BioMed Res. Int. 2015, 356893.
Tao, X.W., Zeng, L.K., Wang, H.Z., Liu, H.C., 2018. LncRNA MEG3 ameliorates respiratory syncytial virus infection by suppressing TLR4 signaling. Mol. Med. Rep. 17, 4138–4144.
Tracy, S., Höfling, K., Pirruccello, S., Lane, P.H., Reyna, S.M., Gauntt, C.J., 2000. Group B coxsackievirus myocarditis and pancreatitis: connection between viral virulence phenotypes in mice. J. Med. Virol. 62, 70–81.
Wang, Y., Li, J., Zhang, L., Sun, H.X., Zhang, Z., Xu, J., Xu, Y., Lin, Y., Zhu, A., Luo, Y., Zhou, H., Wu, Y., Lin, S., Sun, Y., Xiao, F., Chen, R., Wen, L., Chen, W., Li, F., Ou, R., Zhang, Y., Kuo, T., Li, Y., Li, L., Sun, J., Sun, K., Zhuang, Z., Lu, H., Chen, Z., Mai, G., Zhuo, J., Qian, P., Chen, J., Yang, H., Wang, J., Xu, X., Zhong, N., Zhao, J., Li, J., Zhao, J., Jin, X., 2022. Plasma cell-free RNA characteristics in COVID-19 patients. Genome Res. 32, 228–241.
Wang, Y., Wang, P., Zhang, Y., Xu, J., Li, Z., Li, Z., Zhou, Z., Liu, L., Cao, X., 2020. Decreased expression of the host long-noncoding RNA-GM facilitates viral escape by inhibiting the kinase activity TBK1 via S-glutathionylation. Immunity 53, 1168–1181 e1167.
Winkle, M., El-Daly, S.M., Fabbri, M., Calin, G.A., 2021. Noncoding RNA therapeutics - challenges and potential solutions. Nat. Rev. Drug Discov. 20, 629–651.
Wu, Z., Peng, H., Du, Q., Lin, W., Liu, Y., 2015. GYY4137, a hydrogen sulfide-releasing molecule, inhibits the inflammatory response by suppressing the activation of nuclear factor-kappa B and mitogen-activated protein kinases in Coxsackie virus B3-infected rat cardiomyocytes. Mol. Med. Rep. 11, 1837–1844.
Xiang, Y., Zhang, Y., Xia, Y., Zhao, H., Liu, A., Chen, Y., 2020. LncRNA MEG3 targeting miR-424-5p via MAPK signaling pathway mediates neuronal apoptosis in ischemic stroke. Aging 12, 3156–3174 (Albany NY).
Xue, S.T., Zheng, B., Cao, S.Q., Ding, J.C., Hu, G.S., Liu, W., Chen, C., 2022. Long non-coding RNA LINC00680 functions as a ceRNA to promote esophageal squamous cell carcinoma progression through the miR-423-5p/PAK6 axis. Mol. Cancer 21, 69.
Yoon, J.H., Srikantan, S., Gorospe, M., 2012. MS2-TRAP (MS2-tagged RNA affinity purification): tagging RNA to identify associated miRNAs. Methods 58, 81–87.
Yu, Y., Pilgrim, P., Yan, J., Zhou, W., Jenkins, M., Gagliano, N., Bumm, K., Cannon, M., Milzani, A., Dalle-Donne, I., Kast, W.M., Cobos, E., Chiriva-Internati, M., 2008. Protective CD8+ T-cell responses to cytomegalovirus driven by rAAV/GFP/IE1 loading of dendritic cells. J. Transl. Med. 6, 56.
Zhang, J., Liang, Y., Huang, X., Guo, X., Liu, Y., Zhong, J., Yuan, J., 2019. STAT3-induced upregulation of lncRNA MEG3 regulates the growth of cardiac hypertrophy through miR-361-5p/HDAC9 axis. Sci. Rep. 9, 460.
Zhang, L., Yang, Z., Trottier, J., Barbier, O., Wang, L., 2017. Long noncoding RNA MEG3 induces cholestatic liver injury by interaction with PTBP1 to facilitate shp mRNA decay. Hepatology 65, 604–615.
Zhang, Q., Matsuura, K., Kleiner, D.E., Zamboni, F., Alter, H.J., Farci, P., 2016. Analysis of long noncoding RNA expression in hepatocellular carcinoma of different viral etiology. J. Transl. Med. 14, 328.
Zhang, Y., Zhang, H., An, M., Zhao, B., Ding, H., Zhang, Z., He, Y., Shang, H., Han, X., 2018. Crosstalk in competing endogenous RNA networks reveals new circular RNAs involved in the pathogenesis of early HIV infection. J. Transl. Med. 16, 332.
Zheng, C., Wu, S.M., Lian, H., Lin, Y.Z., Zhuang, R., Thapa, S., Chen, Q.Z., Chen, Y.F., Lin, J.F., 2019. Low-intensity pulsed ultrasound attenuates cardiac inflammation of CVB3-induced viral myocarditis via regulation of caveolin-1 and MAPK pathways. J. Cell. Mol. Med. 23, 1963–1975.
Zhu, X., Li, H., Wu, Y., Zhou, J., Yang, G., Wang, W., Kang, D., Ye, S., 2019. CREB-upregulated lncRNA MEG3 promotes hepatic gluconeogenesis by regulating miR-302a-3p-CRTC2 axis. J. Cell. Biochem. 120, 4192–4202.